Performance Bounds of DPSK and OOK for Low Elevation Optical LEO Downlinks

Hennes HENNIGER[1], *Alexandra LUDWIG*[2], *Joachim HORWATH*[2]

[1] German Aerospace Center (DLR), German Remote Sensing Data Center (DFD), 82230 Wessling, Germany
[2]German Aerospace Center (DLR), Institute of Communications and Navigation, 82230 Wessling, Germany

henniger@ieee.org

Abstract. *Optical wireless LEO downlinks are seen as an emerging solution to increase available bandwidth to multi-gigabits per second. One of the biggest challenges is the impact of the atmosphere on the optical signal. The atmosphere causes time-varying link degradation due to index of refraction turbulence, especially at low elevation angles. Since the influence of the turbulence for low elevation downlinks is hardly investigated we perform numerical propagation simulations in order to achieve reliable received signal statistics. These results are further utilized to evaluate performance bounds of optical wireless systems from an information theory perspective. We focus on the two most common optical wireless systems, i.e. NRZ-DPSK and NRZ-OOK. This work shows that under low elevation angles acceptable quality of service can only be reached with high code rates.*

Keywords

Free-space optical communications, channel capacity, index of refraction turbulence, fading, LEO downlink, system performance.

1. Introduction

Optical wireless communications is becoming more and more important in transmission systems. The focus of these links is changing from short-range fixed systems that take advantage of setting up high bandwidth connectivity under fiber-less infrastructure conditions to mobile long-range links or even satellite downlinks. For example, the KIODO (KIrari's Optical Downlink to Oberpfaffenhofen) experiments in 2006 and 2009 have shown the readiness of the optical technology to serve high-rate optical downlinks from low earth orbiting satellite (LEO) [1]. These links can provide an alternative or complement to directional microwave systems with the benefits of optics such as highest data-rates and power efficiency in addition to no frequency interference or regulation problems.

Nevertheless, challenges remain, e.g. the propagation of an optical beam through the atmosphere leads to random variations in phase and amplitude. This is due to turbulence effects caused by fluctuations of the refractive index of the propagation medium as the latter experiences temperature gradients due to solar heating and wind shear. Atmospheric turbulence produces a distorted intensity profile of the beam as well as a distorted phase front, which are both time and space dependent. The intensity fluctuations (called scintillations) result in a fluctuation of the received signal which can significantly reduce the transmission quality. The coherence time is typically in the order of milliseconds while symbol durations at bit rates of interest are shorter than 100 ps.

Several statistical models exist describing the scintillation in satellite downlinks (e.g. [2], [3] and [4]). Besides the log-normal (LN) model [2], [5], [6], [7] which is mainly used under weak turbulence conditions typical for short-range links also several other models are reported in literature, e.g. gamma-gamma [6], [8], [9] or exponential [3]. Most models are not verified to be valid for LEO downlinks under low elevation angles. But especially the operation of the link under low elevation angles is of interest in order to increase the link-duration or downlink-time for a satellite path [10].

On the other hand also several models describing the channel from an information theory perspective do exist: In [11] and [12] the average (ergodic) channel capacity is derived for on-off keying (OOK) systems, whereas we focus in our work on the instantaneous channel capacity instead of the ergodic channel capacity in order to derive link outage probabilities. An analog approach is presented in [13] and [14] also for OOK systems. Anguita et. al. present in their paper [15] a way to evaluate capacity based on the assumption that the variation of the received signal can be seen as a noise process. They focus mainly on the evaluation of horizontal links using OOK.

In this work we are investigating the performance bounds of optical wireless LEO downlinks from an information theory point of view. Thus, two typical modulation schemes are regarded (compare Section 3), i.e. the NRZ (Non-Return-to-Zero)-OOK system and the NRZ-DPSK (differential binary Phase-Shift Keying) system. In Section 2 the statistics of the received signal for low elevation LEO downlinks are developed. As there does not exist

a verified model for LEO downlinks under low elevation angles the received signal statistics are derived from numerical propagation simulation. In addition, the commonly used and well know LN model is presented as well for comparison. The outcomes of Section 2 are used in Section 5 to evaluate the outage probability of the downlink system, while Section 4 reviews the channel capacity in the absence of fading. Finally, concluding comments are provided.

2. Channel Description

A mathematical description of an optical wireless transmission system working over an amplitude-fading channel with output Y is

$$Y = A \cdot X + N \tag{1}$$

where the vector $X \in \mathbb{R}_0^+$ represents generally the transmitted symbols x, $N \in \mathbb{R}$ the signal independent additive noise and $A \in \mathbb{R}^+$ the amplitude variation due to channel influences. (Where $\mathbb{R}$ is the set of real numbers, $\mathbb{R}^+$ is the set of positive real numbers and $\mathbb{R}_0^+$ is the set of positive real number including zero.) Channel loss and channel dynamics are included in the amplitude vector A. A has the probability density function (PDF) $f_{\mathrm{A}}(a)$.

This section is organized as follows: First, the common used LN distribution [2], [5], [6] is presented, that is valid for near zenith downlinks [2]. In the second part, simulations have been done to regard the received amplitude statistics for low elevation angles.

In the following the LN-fading statistics are discussed. The PDF of the received signal A is first modeled by the LN distribution in the case of high elevations:

$$f_{\mathrm{A\,LN}}(a) = \frac{1}{a \cdot \sqrt{2\pi\sigma_{\mathrm{LD}}^2}} \exp\left(-\frac{[\ln a - \mu_{\mathrm{LD}}]^2}{2\sigma_{\mathrm{LD}}^2}\right), a > 0. \tag{2}$$

The parameters of the LN distribution μ_{LD}, σ_{LD}^2 are the mean value and variance of the underlying normal distribution. The expectation value of the LN-PDF $E[A]$ is also the expectation value of the received signal.

$$E[A] = \exp\left(\mu_{\mathrm{LD}} + \frac{\sigma_{\mathrm{LD}}^2}{2}\right) \tag{3}$$

The well known scintillation-index σ_{SI}^2 which is defined by

$$\sigma_{\mathrm{SI}}^2 = \frac{Var[A]}{(E[A])^2}, \tag{4}$$

depends directly on LN variance σ_{LD}^2:

$$\sigma_{\mathrm{SI}}^2 = \frac{\exp(2\mu_{\mathrm{LD}} + \sigma_{\mathrm{LD}}^2)(\exp(\sigma_{\mathrm{LD}}^2) - 1)}{(\exp(\mu_{\mathrm{LD}} + \frac{1}{2}\sigma_{\mathrm{LD}}^2))^2} = \exp(\sigma_{\mathrm{LD}}^2) - 1 \tag{5}$$

and specifies the LN-PDF $f_{\mathrm{A\,LN}}(a)$.

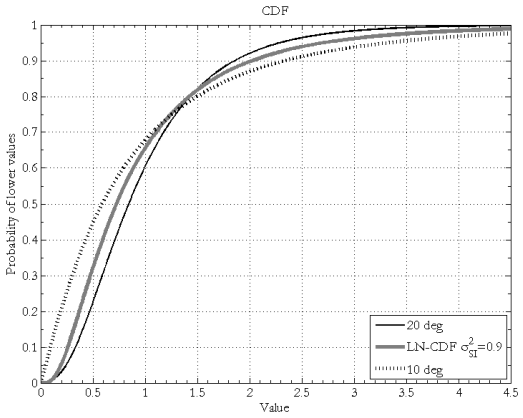

Fig. 1. Normalized cumulative density functions (CDF) for the received signal. The figure shows two simulation results for a 10 deg and a 20 deg elevation LEO downlinks as well as a LN-CDF for comparison.

For low elevation angles the LN model of the received signal statistics which is based on the classical scintillation theory is no longer valid. Several theories extend the validity of the classical scintillation theory from weak to the strong fluctuation regime. These approaches use parabolic or Markov approximation methods. e.g. [16]. Since those scintillation expressions typically contain multifold integrations over infinite domains and require customized and approximate solutions, they are rarely practical for use in engineering analysis [17]. Therefore, the atmospheric wave propagation is simulated numerically for low elevation angles [18]. Here the simulations have been performed with the split-step Fourier method [19] which is based on the paraxial approximation of the wave equation. The two dimensional complex scalar field in the x-y plane is propagated along the propagation (z-) axis. The stochastic index of refraction of the wave equation is applied by the creation of two dimensional phase screens. These random screens are created with an extended version of the Kolmogorov turbulence spectrum and inserted into the propagation path. The propagation distance is divided into N parts with N phase screens and undisturbed vacuum propagation in between. Each phase screen represents a small portion of the inhomogeneous medium confined to a slab. We use the Hufnagel-Valley [20] turbulence profile with $C_{\mathrm{n}}^2 = 1.7 \cdot 10^{-14}\mathrm{m}^{-\frac{2}{3}}$ at sea level and a tropopause wind speed of 21 m/s (HV 5/7). The receiver altitude is set to sea level and the receiver aperture size is much smaller than the intensity speckle size so that no aperture averaging effects have to be taken into account. The results of the simulations show scintillation indexes of about 1.6 for 10 deg elevation and 0.45 for 20 deg elevation. Further simulations result in cumulative density functions (CDF) of the received signal shown in Fig. 1. As it can be seen they differ from the LN-CDF and further especially for the lower elevation angle of 10 deg there is a high probability of very low received signal values i.e. 0.1. That means, that with 10 % probability the power is less than $\frac{1}{10}$ of the mean received power. In comparison in the 20 deg case only 2 % are below $\frac{1}{10}$ of the mean received power. It can be assumed that this behavior

will make reliable communications difficult. All in all the simulations show that in the LEO satellite downlink case the distributions of the received signals depend strongly on the elevation and the LN distribution is not valid for low elevations.

3. Modulation Schemes

In this section we will discuss the behavior of two commonly used modulation schemes. First we will discuss the detection process of an NRZ-OOK receiver. Second an NRZ-DPSK receiver is evaluated.

3.1 NRZ-OOK Receiver

For binary OOK with NRZ symbols the symbols are defined as $x \in \{"H" \to 1, "L" \to 0\}$. Transmit symbol "$H$" means that the transmitter light source is turned on, while "L" means that the light source is switched off. The mean transmit signal is given by $E[X] = \frac{1}{2}$.

The noise N, in (1) models signal independent noise. It is assumed that the receiver performance is dominated by Johnson-Noise (thermal noise), i.e. Gaussian noise statistics are assumed. This assumption can be justified for non optical preamplified receivers, especially for p-i-n diode (positive intrinsic negative diode) receives, where Johnson-Noise of the electrical preamplifier is dominating over the detector noise effects.

For the turbulent channel we assume a block-fading channel model where the amplitude factor a is fixed over a long duration and varies independently over blocks. This means the quality of the output of the system would be constant over a relatively long duration compared to the symbol length. For one fixed amplitude factor $a = const.$ the distributions of the received signal are as follows: The signal independent additive noise N is modeled by the zero-mean Gaussian distribution with variance σ_n^2:

$$f_N(n) = \frac{1}{\sqrt{2\pi\sigma_n^2}} \exp\left(-\frac{n^2}{2\sigma_n^2}\right). \tag{6}$$

Therefore, the PDF for the received signal $f_Y(y|x)$ is given by:

$$f_Y(y|x) = \frac{1}{\sqrt{2\pi\sigma_n^2}} \exp\left(-\frac{[y-\mu_n(x)]^2}{2\sigma_n^2}\right) = \mathcal{N}(\sigma_n^2, \mu_n(x)), \tag{7}$$

where $\mu_n(x)$ represents the mean value for the received symbols "H" or "L" respectively. In order to get an easy mathematical tractability it makes sense to assume that the mean value of symbol "L" equals zero: $E[y|x = "L"] = \mu_n("L") = 0$. Further, it holds according to the definitions made above that for symbol "H" the mean value depends on the amplitude factor a: $E[y|x = "H"] = \mu_n("H") = a \cdot 1$.

Now we define the received signal amplitude S by:

$$S = \mu_n("H") - \mu_n("L"),\ \mu_n("L") < \mu_n("H"). \tag{8}$$

Further we define the quality factor Q as a measure for the quality of the received signal, or the quality of the eye-diagram respectively. We define it as the ratio of a signal to the noise corrupting the signal:

$$Q = \frac{S}{\sigma_n("H") + \sigma_n("L")}. \tag{9}$$

As discussed at the beginning of this section we assume $\sigma_n("L") = \sigma_n("H"), \mu_n("L") = 0$ thus $S = a$ and the Q-factor can be written as

$$Q_{OOK} = \frac{a}{2\sigma_n} \tag{10}$$

for the NRZ-OOK case.

3.2 NRZ-DPSK Receiver

For differential binary Phase-Shift Keying (DPSK) the information is differentially encoded in the phase of the optical signal and decoded with the help of an optical delay interferometer in combination with a balanced receiver [21], [22], [23]. Due to the characteristics of the receiver setup there is always power detected on either of the two photo diodes of the receiver [24]. Thus, the noise of logical one is equal to the noise of a logical zero. The binary send symbols are mapped after the delay interferometer to $x' \in \{+1, -1\}$, with equal noise for both symbols:

$$\sigma_n(+1) = \sigma_n(-1) = \sigma_n. \tag{11}$$

The two states can be found on the constellation diagram at $+1$ and -1, i.e. the received signal amplitude equals $S = 2a$. Therefore, the PDFs of both received signals are equal and analog to the "H"-case of the NRZ-OOK:

$$\begin{aligned} lf_Y(y|x=+1) &= f_Y(y|x=-1) \\ &= \frac{1}{\sqrt{2\pi\sigma_n^2}} \exp\left(-\frac{[y-\mu_n(x)]^2}{2\sigma_n^2}\right) \\ &= \mathcal{N}(\sigma_n^2, \mu_n(x)) \end{aligned} \tag{12}$$

where $\mu_n(x)$ represents the mean value for the symbols: $\mu_n(x=+1) = a$ and $\mu_n(x=-1) = -a$.

The Q-factor for a NRZ-DPSK system is defined by

$$Q = \frac{S}{\sigma_n(+1) + \sigma_n(-1)}. \tag{13}$$

With $S = 2a$ and eq. (11) and (13) the Q-factor in the NRZ-DPSK case becomes

$$Q_{DPSK} = \frac{a}{\sigma_n}. \tag{14}$$

Here no significant phase error is assumed, i.e. the delay-interferometer is always perfectly aligned. In addition no background-light and no amplified spontaneous noise (ASE) are assumed.

It is obvious that for having the same Q-factor as for an NRZ-OOK system, only the half of peak transmitted power is necessary.

In the following, we will have a look at the channel capacity depending on the Q-factor, since this factor is modulation format independent.

4. Conditional Channel Capacity

In this section we evaluate the channel capacity of optical wireless links unaffected by fading. The capacity is given as a function of the time invariant amplitude attenuation a. Generally, the channel capacity C is the maximum achievable rate with that it can be reliably communicated between the transmitter and the receiver [25]. It has the following property:

$$C = \max_{P_X(x)} I(X;Y). \tag{15}$$

$P_X(x)$ denotes the probability of X (vector of sent symbols) to be x, named the distribution of the source symbols. In order to achieve a maximum mutual information $I(X;Y)$, which equals the channel capacity, the source statistics $P_X(x)$ must be matched to the channel statistics. In this work we restrict our source alphabet to the binary case, and the capacity refers to the maximum mutual information using binary source symbols. This represents a binary input and Gaussian (ideal soft-decision) output channel. Further we assume a continuous output alphabet $y \in \mathbb{R}$. According to (1) the channel output Y depends on the channel fading amplitude A. The conditional mutual information for a special channel state $I(X;Y|A=a)$ is defined by:

$$\begin{aligned} I(X;Y|A=a) = & \int_Y \\ & f_{Y|A}(y|"L") \cdot P_X("L") \cdot \log_2 \left(\frac{f_{Y|A}(y|"L")}{\sum_{z="H","L"} P_X(z) \cdot f_{Y|A}(y|z)} \right) \\ & + f_{Y|A}(y|"H") \cdot P_X("H") \cdot \log_2 \left(\frac{f_{Y|A}(y|"H")}{\sum_{z="H","L"} P_X(z) \cdot f_{Y|A}(y|z)} \right) \\ & dy. \end{aligned} \tag{16}$$

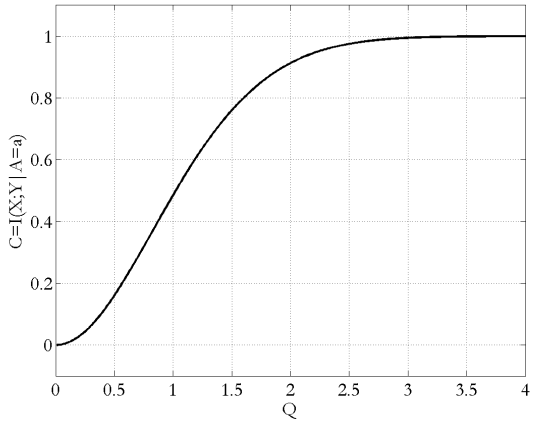

Fig. 2. Conditional channel capacity vs. Q-factor for OOK-NRZ and OOK-DPSK for a binary input Gaussian output channel.

As for the receivers described in this work $f_Y(y|x = "L")$ and $f_Y(y|x = "H")$ have equal shape $\mathcal{N}(\sigma_n^2, \mu_n(x))$, the source statistic which maximizes the mutual information is given by $P_X(x = "H") = P_X(x = "L") = \frac{1}{2}$.

So one gets the conditional mutual information or conditional channel capacity respectively for a fixed $A = a$:

$$\begin{aligned} I(X;Y|A=a) = & \tfrac{1}{2} \int_Y \\ & f_{Y|A}(y|x="L") \cdot \log_2 \left(\frac{2\, f_{Y|A}(y|x="L")}{f_{Y|A}(y|x="L") + f_{Y|A}(y|x="H")} \right) \\ & + f_{Y|A}(y|x="H") \cdot \log_2 \left(\frac{2\, f_{Y|A}(y|x="H")}{f_{Y|A}(y|x="L") + f_{Y|A}(y|x="H")} \right) \\ & dy \end{aligned} \tag{17}$$

where $f_{Y|A}(y|x)$ is $\mathcal{N}(\sigma_n^2, \mu_n(x))$ with $\mu_n(x)$ being 0, a for OOK or $-a$ and $+a$ for DPSK. The conditional channel capacity can be evaluated as a function of $Q(a)$ by numerical integration, e.g. using tools like MatLab. The result is plotted in Fig. 2. It can be seen that for $Q > 3$ the mutual information converges to its maximum of 1 bit / channel use. The $C(Q)$-function is equal for NRZ-OOK and NRZ-DPSK because of the definition of Q made above.

5. Fading Channel Outage Probability

In this section, the channel outage probability for the different statistics of the received signal is regarded.

We define the (code) rate R which states what portion of the total amount of information is useful. In forward error correction the encoder generates for every k source symbols a code word with total n codes symbols, of which $n-k$ are redundant.

$$R = \frac{k}{n} \leq 1 \tag{18}$$

The channel coding theorem states that there exist codes with rate $C > R$ which enable transmission with arbitrary small error probability (error-free). Practically finite length codes will have a nonzero probability of error, however, good finite length codes approaching Shannon's capacity have been found. No such codes exist for $C < R$.

If fading occurs, that means $a \neq const.$ there is a non zero probability that the instantaneous channel capacity is temporarily below the transmitted time invariant rate R_0, i.e. in fades Q decreases temporarily and the following holds: $C(Q) < R_0$. In this case a link outage occurs. An outage is defined as an event where the instantaneous capacity of the channel is below the time invariant rate. For a given fixed rate R_0, the probability of outage p_B is denoted as

$$p_B(R_0) = \Pr\left[C(a) < R_0\right]. \tag{19}$$

Considering the monotonic increase of $C(.)$ with a, the above equation can be rewritten as follows [14]:

$$p_B(R_0) = \Pr\left[a < a_0\right], \tag{20}$$

where the threshold a_0 is given by condition

$$I(X;Y|A=a_0)=R_0. \tag{21}$$

The probability of outage is the CDF of a evaluated at a_0 and can be expressed as:

$$p_{\mathrm{B}}=\int_0^{a_0} f_{\mathrm{A}}(a)\,\mathrm{d}a. \tag{22}$$

If we assume that $f_{\mathrm{A}}(a)$ follows a simple LN distribution from (2) and assuming normalized values $E[A]=1$ the outage probability equals

$$p_{\mathrm{B}}=\frac{1}{2}\left(1+\mathrm{erf}\left[\frac{\ln a_0-\mu_{\mathrm{LD}}}{\sqrt{2\sigma_{\mathrm{LD}}^2}}\right]\right). \tag{23}$$

Using (3) and (5) the outage probability becomes

$$p_{\mathrm{B}}(a_0,\sigma_{\mathrm{SI}}^2)=\frac{1}{2}\left(1+\mathrm{erf}\left[\frac{\ln(a_0\sqrt{\sigma_{\mathrm{SI}}^2+1})}{\sqrt{2\ln(\sigma_{\mathrm{SI}}^2+1)}}\right]\right). \tag{24}$$

For a certain scintillation index σ_{SI}^2 which characterizes the dynamics of the received signal and using equations (21) and (24) the outage probability p_{B} can be given as a function of rate R_0.

In analogy to the LN distribution the CDFs of the outage probability in the LEO downlink case under low elevation angles (10 deg and 20 deg) have been evaluated. The CDFs are shown in the Fig. 1. As the numerically calculated CDFs do not show a closed form for the determination of p_{B}, see (23) they were fitted piecewise and subsequently for the calculation of the outage probability p_{B} according to (22) and (21). In addition it must be said that the simulated CDFs could not be fitted with standard assumed statistics like LN, gamma-gamma or exponential with an acceptable overall fitting-error.

Outage probabilities are shown in Figs. 3 and 4 respectively. They show the theoretical bound of possible outage probabilities for a certain rate and a certain Q-factor. In practical implementations, i.e. for a certain rate, only outage probabilities greater than the bounds are possible.

Discussion of the plots shown in Figs. 3 and 4: In the case of no fading ($\sigma_{\mathrm{SI}}^2\to 0$) the receiver's thermal noise defines the channel capacity and the maximum rate for error-free transmission, respectively. In the plots the rate is set equal to the channel capacity ($C=R$) for the mean received power. This rate depends on the quality factor Q given for the mean received signal. Because of fading there is a non zero probability that Q is temporarily reduced. That means that if one is transmitting with constant rate the channel capacity is temporarily below the rate ($C<R$). Therefore outages take place with a certain probability. It can be observed in the plots that for a constant rate the channel degradation increases with stronger fading (larger values of σ_{SI}^2). It has to

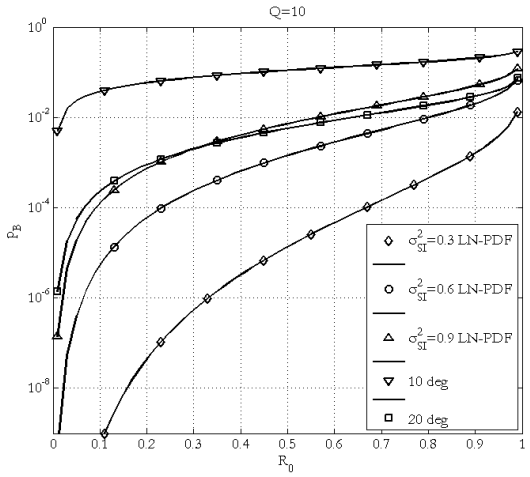

Fig. 3. Outage probability as function of code rate. The Q-factor of the receiver in the absence of fading is set to 10. Several fading characteristics are given: LN-fading and simulation results for 10 deg and 20 deg elevation LEO downlink.

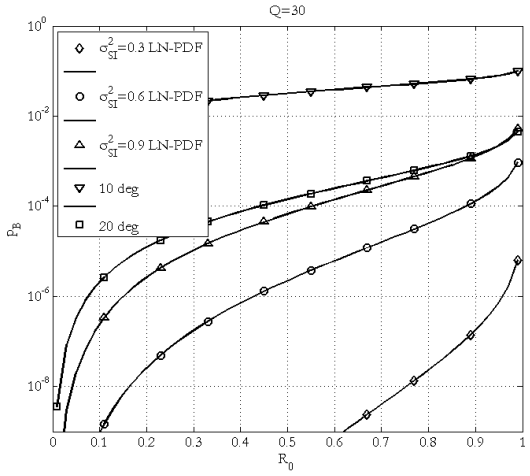

Fig. 4. Same as Fig. 3 but with larger link margin $Q=30$.

be seen that for the given Q-values of 10 and 30 the channel capacity for a channel without fading would have been almost 1 bit/channel use which means that an error-free transmission would have been possible. Nevertheless, due to the fading it can be observed that with non-adaptive code rates there might be always a non-zero probability of outage.

Further, it can be seen that regarding the outage probability the LN model of the received power, which is typically used for high elevation angles, also shows outage probabilities in the same order of magnitude as the simulated statistics for low elevation angles, if large scintillation indices are assumed.

Furthermore, it can be observed that for low elevation angles (10 deg) reliable communication is possible, but only at the cost of spending a lot of overhead for the error correcting code. This is well-founded in the CDF (compare Fig. 1) which shows a high probability of low values for the 10 deg link.

6. Conclusion

In this work we evaluated the performance of NRZ-OOK and NRZ-DPSK optical satellite downlinks especially under low elevations. Received signal statistics for low elevation angles have been investigated in detail with the help of numerical simulations and compared with the LN model. The simulated statistics differ from the LN distribution.

According to these statistics the outage probability of an optical wireless communication system was derived depending on the code rate. It has been shown that communication links under low elevation angles are very restricted in terms of outage probability with code rates typically used for communication systems, but with sufficient overhead communication is nevertheless possible.

References

[1] PERLOT, N., KNAPEK, M., GIGGENBACH, D., HORWATH, J., BRECHTELSBAUER, M., TAKAYAMA, Y., JONO, T. Results of the optical downlink experiment KIODO from OICETS satellite to optical ground station oberpfaffenhofen (OGS-OP). In *Free-Space Laser Communication Technologies XIX*. San Jose (USA), 2007.

[2] ANDREWS, L. C., PHILLIPS, R. L., HOPEN, C. Y. *Laser Beam Scintillation with Applications*. SPIE Optical Engineering Press, 2001.

[3] ANDREWS, L. C., PHILLIPS, R. L. *Laser Beam Propagation through Random Media, Second Edition*. SPIE Press Monograph Vol. PM152, 2005.

[4] YURA, H. T., MCKINLEY, W. G. Optical scintillation statistics for IR ground-to-space laser communication systems. *Applied Optics*, 1983, vol. 22, no. 21, p. 3353 – 3358.

[5] GIGGENBACH, D., HENNIGER, H. Fading-loss assessment in atmospheric free-space optical communication links with on-off keying. *Optical Engineering*, 2008, vol. 47.

[6] VETELINO, F. S., YOUNG, C., ANDREWS, L. Fade statistics and aperture averaging for gaussian beam waves in moderate-to-strong turbulence. *Applied Optics*, 2007, vol. 46, no. 18, p. 3780 – 3789.

[7] HENNIGER, H., EPPLE, B., HAAN, H. Maritime mobile optical-propagation channel measurements. In *Proceedings of IEEE International Conference on Communications 2010*. Cape Town (South Africa), 2010.

[8] AL-HABASH, M., ANDREWS, L., PHILLIPS, R. Mathematical model for the irradiance probability density function of a laser beam propagating through turbulent media. *Optical Engineering*, 2001, vol. 40, p. 1554 – 1562.

[9] ANDREWS, L. C., PHILLIPS, R. L., HOPEN, C. Y., AL-HABASH, M. A. Theory of optical scintillation. *Journal of the Optical Society of America A*, 1999, vol. 16, no. 6, p. 1417 – 1429.

[10] GIGGENBACH, D., HORWATH, J., EPPLE, B. Optical satellite downlinks to optical ground stations and high-altitude platforms. In *16th Mobile and Wireless Communication Summit.* Budapest (Hungary), 2007, p. 1 – 4.

[11] NISTAZAKIS, H., KARAGIANNI, E., TSIGOPOULOS, A., FAFALIOS, M., TOMBRAS, G. Average capacity of optical wireless communication systems over atmospheric turbulence channels. *Journal of Lightwave Technology*, 2009, vol. 27, no. 8, p. 974 – 979.

[12] SANDALIDIS, H., TSIFTSIS, T. Outage probability and ergodic capacity of free-space optical links over strong turbulence. *Electronics Letters*, 2008, vol. 44, no. 1, p. 46 – 47.

[13] FARID, A., HRANILOVIC, S. Channel capacity and non-uniform signalling for free-space optical intensity channels. *IEEE Journal on Selected Areas in Communications*, 2009, vol. 27, no. 9, p. 1553 – 1563.

[14] FARID, A. A., HRANILOVIC, S. Outage capacity optimization for free-space optical links with pointing errors. *Journal of Lightwave Technology*, 2007, vol. 25, no. 7, p. 1702 – 1710.

[15] ANGUITA, J., DJORDJEVIC, I., NEIFELD, M., VASIC, B. Shannon capacities and error-correction codes for optical atmospheric turbulent channels. *Journal of Optical Networking*, 2005, vol. 4, no. 9, p. 586 – 601.

[16] KLYATSKIN, V. I., TATARSKI, V. I. The parabolic equation approximation for propagation of waves in a medium with random inhomogeneities. *Sov. Phys. JETP31*, 1970, p. 335 – 339.

[17] BAKER, G. J. Gaussian beam weak scintillation: low-order turbulence effects and applicability of the Rytov method. *Journal of the Optical Society of America A*, 2006, vol. 23, no. 2, p. 395 – 417.

[18] HORWATH, J., PERLOT, N. Determination of statistical field parameters using numerical simulations of beam propagation through optical turbulence. *Proc. of SPIE*, 2004, vol. 5338.

[19] FLECK, J. F. M. Time-dependent propagation of high energy laser beams through the atmosphere. *Applied Physics*, 1976, vol. 10, no. 2, p. 129 – 160.

[20] ANDREWS, L. C., PHILLIPS, R. L. *Laser Beam Propagation through Random Media*. SPIE Press, 1998.

[21] AGRAWAL, G. P. *Fiber-Optic Communication Systems*. Wiley, 2002.

[22] GNAUCK, W. Optical phase-shift-keyed transmission. *Journal of Lightwave Technology*, 2005, vol. 23, no. 1, p. 115 – 130.

[23] GNAUCK, A. H., RAYBON, G., BERNASCONI, P. G., LEUTHOLD, J., DOERR, C. R., STULZ, L. W. 1-Tb/s (6x170.6Gb/s) transmission over 2000-km NZDF using OTDM and RZ-DPSK format. *IEEE Photonics Technology Letters*, 2003, vol. 15, no. 11, p. 1618 – 1620.

[24] SINSKY, J. H., ADAMIECKI, A., GNAUCK, A., BURRUS, C., LEUTHOLD, J., WOHLGEMUTH, O., UMBACH, A. 42.7 Gb/s integrated balanced optical front end with record sensitivity. In *Optical Fiber Communications Conference*. Atlanta (USA), 2003.

[25] SHANNON, C. E. A mathematical theory of communications. *Bell Syst. Tech. J.*, 1948, vol. 27, p. 379 – 423.

About Authors...

Hennes HENNIGER was born in 1978 in Berlin. He received his Dipl.-Ing. degree from the University of Applied Sciences, Munich, in 2002, and his Master of Science degree in 2004. He joined the Optical Communications Group of the German Aerospace Center (DLR) in 2001. He was project manager of the mobile near ground optical demonstrator project and of the Kirari Optical Downlink to Oberpfaffenhofen (KIODO) LEO satellite downlink project 2009. His current research interests are channel modeling and error protection techniques to overcome fading in free-space optical communications. Since 2010 he is with the German Re-

mote Sensing Data Center (DLR-DFD). In 2007 he founded the Codex consulting and development company. Henniger has served as a program committee member for the SPIE's conference on free-space laser communications at the Optics and Photonics symposium since 2008. In 2010 he was guest editor of the Special Issue on Free-space Optical Communications of the Radioengineering Journal. Henniger is a Member of IEEE.

Alexandra LUDWIG received her Dipl.-Ing in electrical engineering and information technology from the Karlsruhe Institute of Technology (KIT), Karlsruhe, Germany in 2008. Since 2008 she is a Ph.D. student at the Institute of Communications and Navigation of the German Aerospace Center (DLR), where she is researching high-speed free-space optical communication systems with high sensitivity.

Joachim HORWATH received a Dipl.-Ing. (MSc) degree in electrical engineering from the University of Graz, Austria, in 2002. Since 2002 he is a staff member of the Institute of Communications and Navigation at the German Aerospace Center (DLR). He managed several research projects focusing on free-space optical communication for HAP satellite and avionic applications and is responsible for the development of optical terminals. His research interests are focused on atmospheric turbulence effects on coherent and incoherent optical communication links and numerical simulation of turbulent wave propagation.